Novel Device of CO Adsorption on Degradable Cellulose-Based Strips

Man Singh,[1] Suman Yadav,[1] Sharif Ahmed[2]

[1]*Chemistry Research Lab, Deshbandhu College, University of Delhi, New Delhi 110019, India*
[2]*Chemistry Department, Jamia Millia Islamia, New Delhi 110025, India*

Received 19 September 2002; accepted 11 April 2003

ABSTRACT: An antipolution polymer strip (APPS) was designed using a cellulose strip (8 × 3 cm) coated with disinfectant polymer resin followed by impregnation with transitional metals (100 μm each). The present studies focused primarily on protection of animals, especially humans, from carbon monoxide (CO) present in the atmosphere because of incomplete combustion of fuel from motor vehicles. Diffusion of atmospheric CO gas causes air pollution. Human blood absorbs CO from the atmosphere, resulting in breathing difficulty and various other ailments. The investigation confirmed that APPS adsorbs CO, thereby providing some protection for living beings. © 2003 Wiley Periodicals, Inc. J Appl Polym Sci 91: 678–685, 2004

Key words: adsorption; antipollution; diffusion; van der Waals force; disinfectant polymer resin

INTRODUCTION

As early as 1773 the process of gas adsorption was carried out, first on wood charcoal then, later, on other porous materials found in nature such as rocks and soil, and even on used building materials. Progressively, experiments were conducted with adsorbents such as silica gel, sodium sulfate, alumina, and $CaSiO_3$; still later studies were carried out under van der Waals forces. Qualitative techniques were followed by quantitative methods in which factors like temperature, pressure, nature of adsorption enthalpy and entropy monitor the process.

Hydrocarbon, coal, and petroleum products are used as fuel in transportation, throughout industry, and in such applications as domestic cooking stoves, resulting in emission of CO, NO, NO_2, SO_2, and sulfur dust. Among the polluting gases CO is highly toxic. To protect humans from harmful gases it is necessary to develop materials that preserve and protect life, particularly in pollution-prone metropolitan areas of India. To prepare antipollution polymer strip (APPS) materials we considered use of cellulose waste, rice husk, and metals such as Ni, Cr, and Zn dust. To investigate the interface property of APPS photoelectron spectroscopy was used. APPS may be pasted strategically on automobiles, advertising board banners, gates, windows, and in various locations throughout different industries to reduce atmospheric CO. It may be useful to mix antipollution polymers with surface coatings such as paint and varnishes to protect from CO toxic gases. Present studies are being carried out for the application to industries so that the pollution from industrial gases and vehicle emissions, to name several leading sources, are minimized.

Correspondence to: M. Singh.
Contract grant sponsor: UGC, New Delhi, India.

Journal of Applied Polymer Science, Vol. 91, 678–685 (2004)

EXPERIMENTAL

Mathematical support

Freundlich and Kroeker (1892; cited in Glasston[1]) proposed the relation

$$x/m = kp^{1/n} \tag{1}$$

where x and m are the weights of adsorbate and adsorbent, respectively; p is constant pressure; k and n are experimental constants for a particular temperature, where $(1/n) < 1$ distinguishes adsorption from distribution formulated by Henry (cited in Borrow[9]). The log of eq. (1) gives the following relation:

$$\log x/m = \log k + (1/n)\log p \tag{2}$$

Willard Gibbs (1878), Thomson (1888), Langmir[1] (1916) and Bain (1926–1929) studied the unimolecular layer of CO adsorption on wood charcoal, and van der Waals forces[10] were ascribed to explain the multimolecular layer at prescribed temperature and pressure. Surfaces of glass, mica,[11,12] platinum, and mercury were also characterized by a unimolecular layer at low pressure from the following relationships:

$$(1 - \theta) \propto \alpha \tag{3}$$

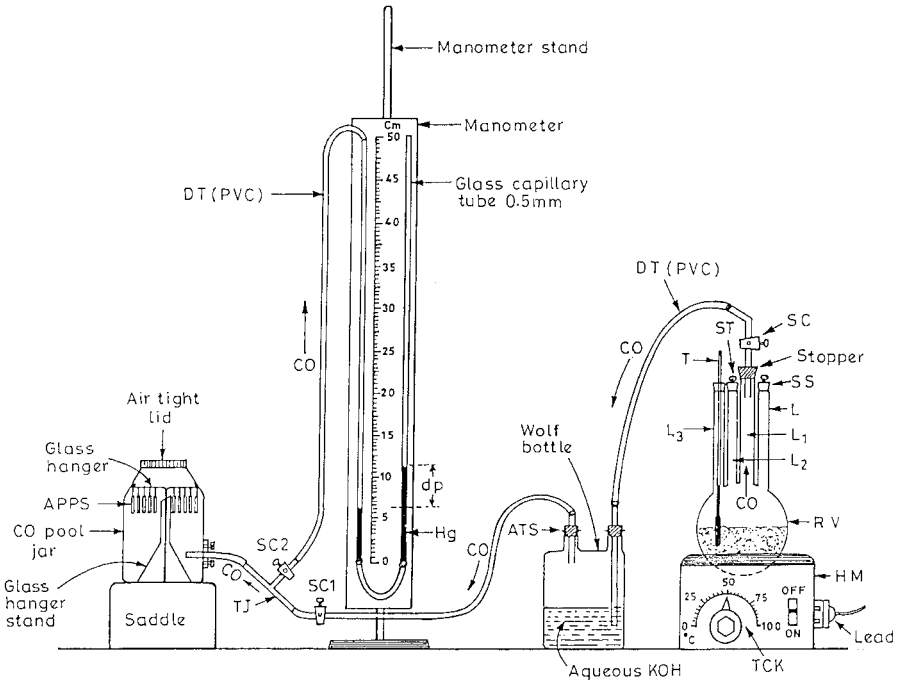

Figure 1 Sketch diagram of operational unit for CO adsorption. Abbreviations: HM, heating mantle; TCK, temperature-controlling knob; RV, reaction vessel; L, L_1, L_2, L_3, limbs; SS, safety stopper; SC, stopcock; ST, sample tube; T, thermometer; DT, delivery tube; ATS, airtight stopper; SC1, SC2, stopcocks; TJ, T junction; dp, differential pressure.

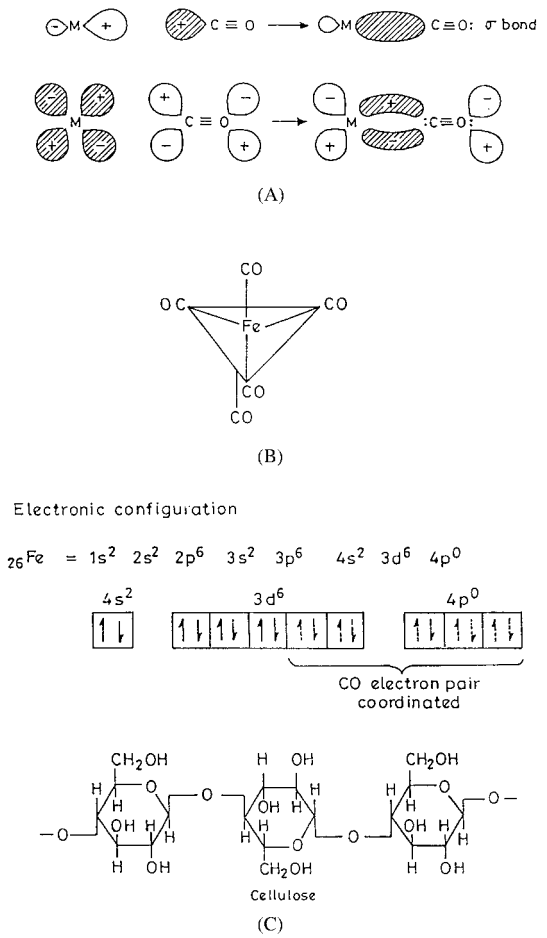

$$\mu = \nu\theta \tag{4}$$

where μ is the number of molecules striking 1 cm^2 of surface, α and ν are constants for a given gas, θ is the fraction of total available surface area for adsorption, and $1 - \theta$ is the unabsorbed surface area for rate determination derived from

$$(1 - \theta) \propto \mu \tag{5}$$

where $\propto \mu$ is the number of molecules adhering to each 1 cm^2 of surface/s.

The kinetic theory of gases[13] monitors adsorption as expressed in the following relation:

$$F(v)\,dv = 4\pi\left(\frac{m}{2\pi kT}\right)^{3/2} e^{-mv^2/kt} v^2\,dv \tag{6}$$

where v is velocity, m is mass, k is the Boltzmann constant, T is the temperature, and dv represents the variation in velocity. CO collides onto the metal surface causing a heavier collision complex of high den-

Figure 2 (A) Backbonding dative π bond from full d orbital on central metal atom M to empty p orbital on C atom of carbonyl. (B) Trigonal bipyramidal structure of iron carbonyl $Fe(CO)_5$ formed by CO adsorption on APPS. (C) Structure of cellulose used for APPS preparation.

TABLE I
Amount of CO Adsorbed on APPS at Different Interval of Time Under Same Experimental Conditions[a]

	Set 1 (metal wt = 0.0500 g, t = 2 h)			Set 2 (metal wt = 0.0500 g, t = 2.30 h)			Set 3 (metal wt = 0.0500 g, t = 3 h)		
	wt. BA	wt. AA	wt. CA	wt. BA	wt. AA	wt. CA	wt. BA	wt. AA	wt. CA
ZOS									
Ti	0.1996	0.1999	0.0003	0.1996	0.1999	0.0003	0.1883	0.1886	0.0003
Cr	0.2525	0.2535	0.0010	0.6371	0.6431	0.0060	0.5603	0.5618	0.0015
Fe	0.1857	0.1858	0.0001	0.6100	0.6184	0.0084	0.6210	0.6772	0.0562
CO	0.1102	0.1996	0.0894	0.6275	0.6347	0.0072	0.5250	0.5640	0.0390
Ni	0.2107	0.2217	0.0110	0.6718	0.6751	0.0033	0.5750	0.6920	0.1170
Zn	0.2341	0.2347	0.0006	0.2051	0.2057	0.0006	0.2051	0.2057	0.0006
SOS									
Ti	0.1365	0.1369	0.0004	0.1365	0.1369	0.0004	0.1426	0.1428	0.0002
Fe	0.5107	0.6552	0.1445	0.5107	0.5520	0.0413	0.5107	0.6552	0.1445
Ni	0.1771	0.1778	0.0007	0.6354	0.6491	0.0137	0.5720	0.6100	0.0380
Cu	0.1604	0.1607	0.0003	0.6295	0.6323	0.0028	0.6127	0.6611	0.0484
Zn	0.2037	0.2038	0.0001	0.2826	0.2829	0.0003	0.2826	0.2827	0.0001
TOS									
Cr	0.1596	0.1599	0.0003	0.7079	0.7091	0.0012	0.5930	0.6240	0.0310
Fe	0.0501	0.0509	0.0001	0.5954	0.5991	0.0037	0.5420	0.5540	0.0120
DOS									
Fe^0	0.0504	0.0508	0.0004	0.6100	0.6184	0.0084	0.6210	0.6772	0.0562
Fe^{2+}	0.0506	0.0508	0.0002	0.5107	0.5520	0.0413	0.5107	0.6552	0.1445
Fe^{3+}	0.05008	0.0509	0.0001	0.5954	0.5991	0.0037	0.5420	0.5540	0.0120
Ti^0	0.1996	0.1999	0.0003	0.1996	0.1999	0.0003	0.1883	0.1886	0.0003
Ti^{2+}	0.1365	0.1369	0.0004	0.1365	0.1369	0.0004	0.1426	0.1428	0.0002
Cr^0	0.2525	0.2535	0.0010	0.6371	0.6431	0.0060	0.5603	0.5618	0.0015
Cr^{3+}	0.1596	0.1599	0.0003	0.7079	0.7091	0.0012	0.5930	0.6240	0.0310
Ni^0	0.2107	0.2217	0.0010	0.6718	0.6751	0.0033	0.5750	0.6920	0.1170
Ni^{2+}	0.1771	0.1778	0.0007	0.6354	0.6491	0.0137	0.5720	0.6100	0.0380
Zn^0	0.2341	0.2347	0.0006	0.2051	0.2057	0.0006	0.2051	0.2057	0.0006
Zn^{2+}	0.2037	0.2038	0.0001	0.2826	0.2829	0.0003	0.2826	0.2827	0.0001

[a] wt. BA, weight before adsorption; wt. AA, weight after adsorption; wt. CA, weight of CO adsorbed on processed strip; t, time of metal exposure for CO adsorption; ZOS, zero oxidation state; SOS, secondary oxidation state; TOS, tertiary oxidation state; DOS, different oxidation state.

sity that becomes established on the surface, thus requiring the application of collision theory. Diameter σ and speed v in time t define the collision frequency as

$$\text{Collision frequency} = \pi\sigma^2 v n^* \qquad (7)$$

where n^* is the density of molecules. Under van der Waals investigation, the cellulose strip does interact with the covalent bond and the intermolecular, adhesive, and vacant forces of metals. The use of cellulose fibers with *N*-methyl morpholine *n*-oxide (NMMO) by Karlsson and Blachot[14] and Johan and Gatenholm[15] for high surface properties and tensile strength supports our model. Gasteiger et al.[17–20] investigated CO (coordinate bond[16]) oxidation on Pt–Ru electrode surfaces, which supported the bifunctional kinetic model based on Monte Carlo[21] simulations, such as the effect that oxygen over potential CO also has on oxidation.[21] The techniques require an expensive infrastructure but we simplified the process to keep within the experimental level approach involving minimal infrastructure and easily available resources (e.g., uncured MDUF polymer resin prepared by polycondensation). Emission[22] of CO was estimated by use of carbon isotope in methane and oxidation with known isotopes of oxygen number.[23] Estimation[18,22] of methane oxidation[26,27] was similarly carried out by Logan et al.[24] and Seiler et al.[25] Watanabe and Zhu[28] studied electrocatalytic oxidation of CO on Pt–Fe alloy, Pt–Co, and Pt–Mo by X-ray. A number of investigators[35–42] made composites of polyvinyl chloride and hard wood (aspen) in combination with saw dust; and Bataille et al.[43] used cellulose fiber of low weight, low gravimetric density, low abrasion, and the least damaging in reinforcement[44] of the substrate.

Preparation of APPS

MDUF resin-coated cellulose strip (8 × 3 cm) was impregnated with nearly 0.05 mg of transitional metal and dried under vacuum in a desiccator containing P_2O_5. Dried APPS was checked for the absence of

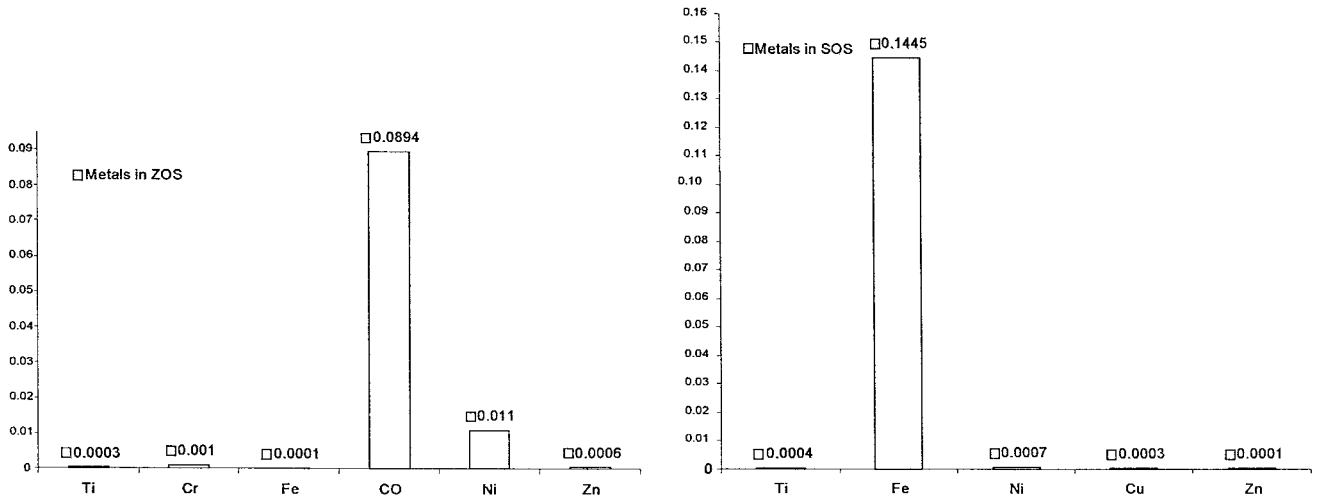

Figure 3 Amount of CO adsorbed in grams (y-axis) and metals with zero oxidation state (x-axis). Data written over bars represent amount of CO adsorbed.

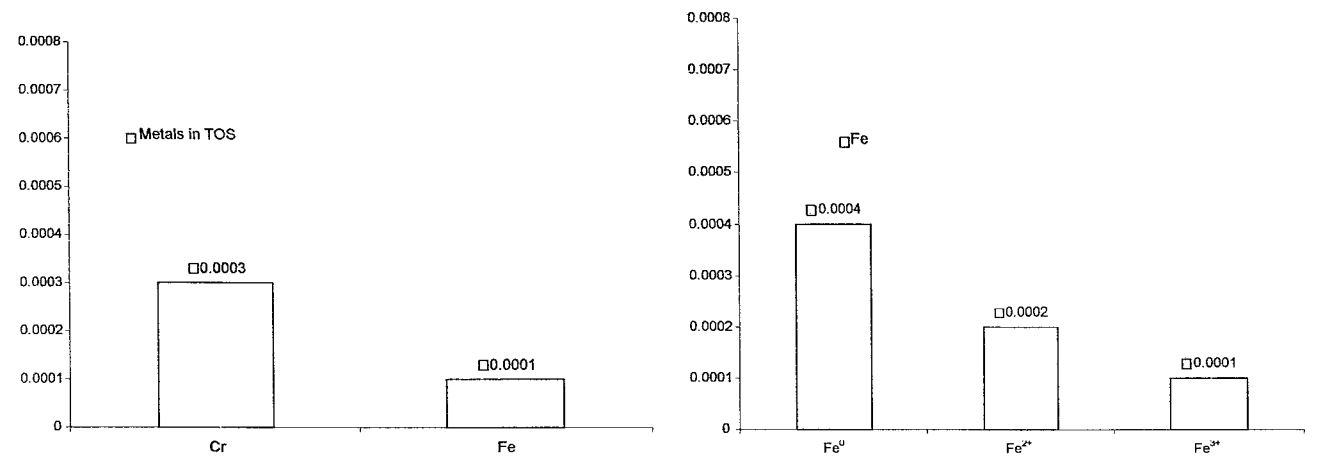

Figure 4 Amount of CO adsorbed in grams (y-axis) and metals with zero oxidation state (x-axis). Data written over bars represent amount of CO adsorbed.

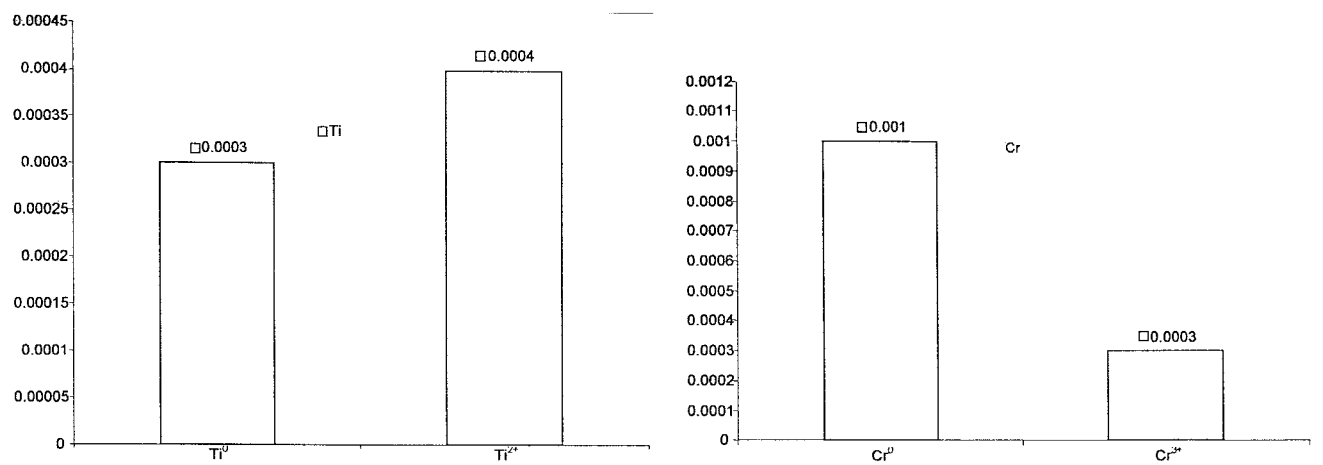

Figure 5 Amount of CO adsorbed in grams (y-axis) and metals with zero oxidation state (x-axis). Data written over bars represent amount of CO adsorbed.

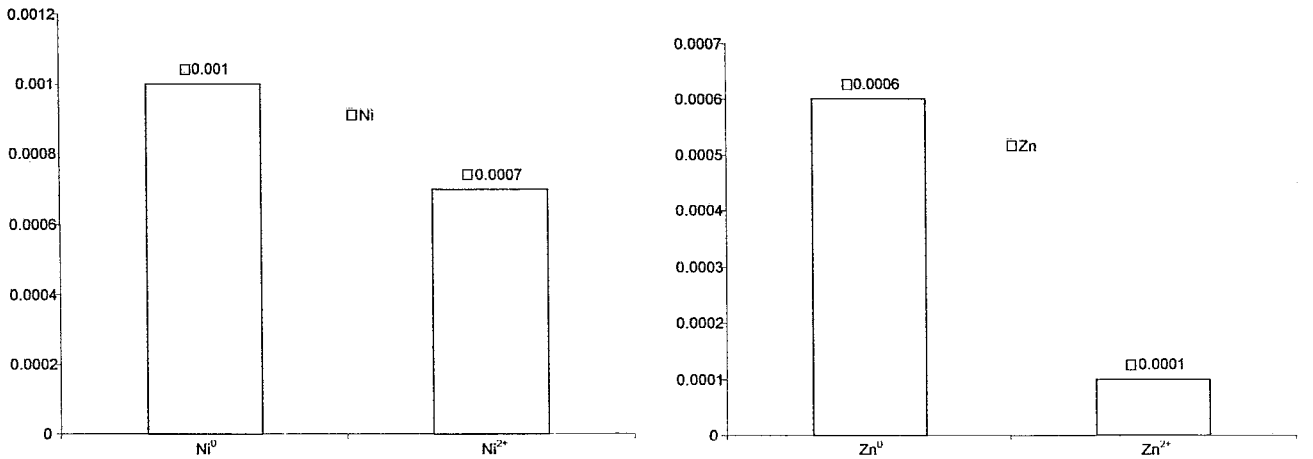

Figure 6 Amount of CO adsorbed in grams (y-axis) and metals with zero oxidation state (x-axis). Data written over bars represent amount of CO adsorbed.

moisture with anhydrous $CuSO_4$ in desiccator (Fig. 1). The structure of cellulose used for APPS preparation is shown in Figure 2.

Preparation of carbon monoxide

Carbon monoxide was prepared using oxalic acid and concentrated H_2SO_4 at 75°C in a four-neck round-bottom flask (Fig. 1). The resin and metal-coated APPS were weighed (Table I) and placed in an airtight jar (Fig. 1). CO was passed through a solution of 5–10% of potassium hydroxide (free from CO_2) for variable periods of 2.00, 2.30, and 3.00 h, after which APPS were again weighed. There was an increase in weight (Table I), indicating that APPS adsorbed CO. The adsorption of CO on APPS was confirmed by X-ray florescence (XRF) and SEM techniques (see Fig. 2).

RESULTS AND DISCUSSION

Ti, Cr, Fe, Co, Ni, Cu, and Zn metals were selected for CO adsorption at 29°C. The weight of adsorbed CO for various times was plotted against metals shown in Figures 3–6 and the values are given in Table I. Each metal was plotted against time and oxidation states with increasing number of electrons (Figs. 3–6). It was further confirmed by conducting the experiment again. The first set of experiments was run for 2 h where cobalt with zero oxidation state (ZOS) recorded the maximum adsorption; Ni and Cr adsorbed almost the same amount of CO; whereas sulfate salt of titanium and zinc adsorbed the least. Ni in the second oxidation state (SOS) showed greater CO adsorption than that of metal salts of Ti, Fe, and Cu. Among sulfate salts of chromium and iron with third oxidation state, chromium recorded higher adsorption.

Freshly prepared APPS (under identical conditions) were exposed to CO vessel for 2.00, 2.30, and 3.00 h. Ti and Zn of ZOS showed identical adsorption, even after increasing the exposure time, whereas adsorption by Cr, Fe, and Ni of ZOS increased with increasing exposure time; however, in the case of Co (cobalt), adsorption initially de-

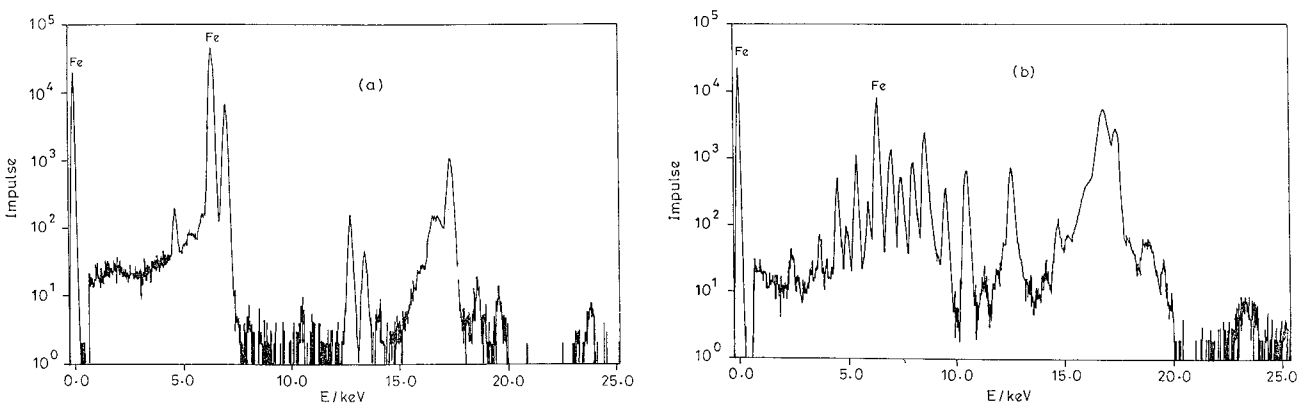

Figure 7 X-ray fluorescence (XRF) spectra with pure Fe powder: (a) before CO adsorption; (b) after CO adsorption.

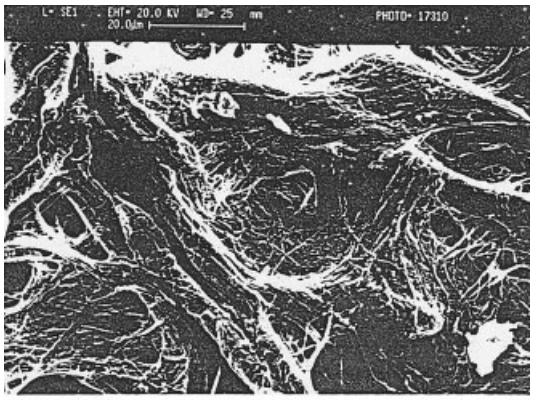

(a)

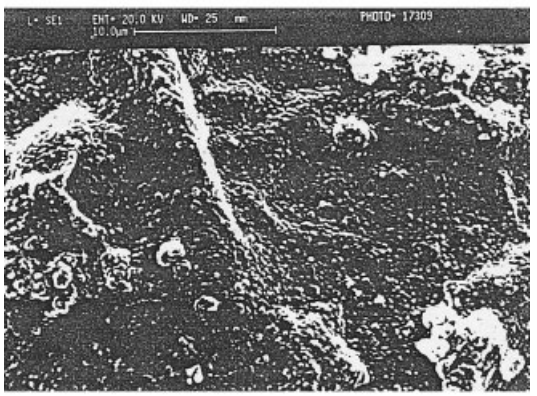

(b)

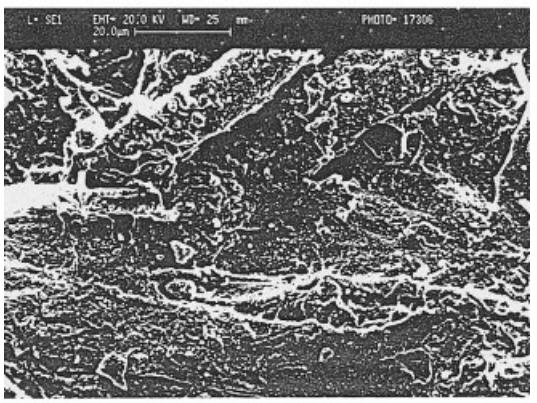

(c)

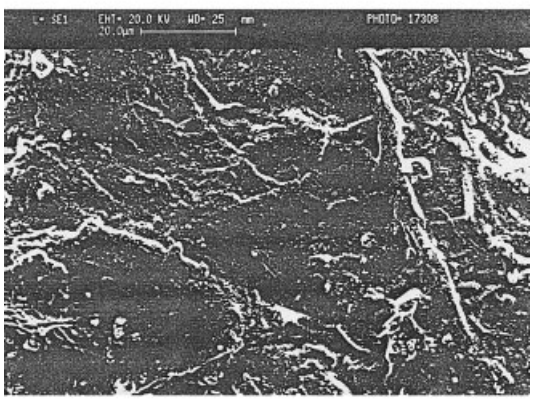

(d)

creased then increased with time. Ti in SOS showed no change up to 2.30 h but adsorption increased significantly when it reached 3.00 h, which may be the result of physical forces caused by the adhesive and cohesiveness by accumulated gas pressure. Cu and Zn in SOS increased adsorption with time, whereas in Fe adsorption initially decreased than increased. In Ni in SOS adsorption first increased than decreased with time, whereas in the case of Cu and Zn adsorption increased with time. The adsorption was confirmed as stated in the text.

XRF spectroscopy

XRF spectra[45] were recorded with a Model X-lab 2000 (Spectro, Germany). Before CO adsorption pure iron of half-filled 3 d orbital and completely empty 4 p orbital facilitates a maximum scintillation, causing an impulse of electrons of 5.25×10^4 counts/s. After adsorption the orbitals are completely filled as CO donates a coordinate pair of electrons to Fe to form a carbonyl complex. It resists the free scintillation or impulse of electrons resulting in impulse decreases to 40.25×10^3 count/s [shown in Fig. 7(b)]. These results further confirm that the adsorption of CO on iron is a chemical process, which is also true for the chosen transition metals.

SEM studies

Electromicrographs of resin-coated and metal-impregnated cellulose strips shown in Figure 8(a)–(d) were recorded with a Cambridge stereo scan S-360 at a resolution of 3000 μm at 11.5 cm, with a silver coating (thickness 100–200 Å). Resin SEM micrographs reveal strong networking between resin and cellulose where the cracks and wider furrows are substantially reduced in number. The white inclined patches and horizontal stacks of impregnated APPS disappear on adsorption and SEM of unabsorbed APPS differs from that of adsorbed by the presence of large diffused patches, thereby confirming the presence of metal complexes.

IR studies

The IR are recorded in Figure 9(B), which represents spectra of polymer resin (MDUF) in water, and the intrinsic viscosity of the solution fits the Mark–Hou-

Figure 8 SEM micrographs: (a) pure cellulose strip; (b) cellulose strip coated with polymer resin; (c) cellulose strip coated and impregnated with resin and metal before adsorption; (d) cellulose strip coated and impregnated with resin and metal after adsorption.

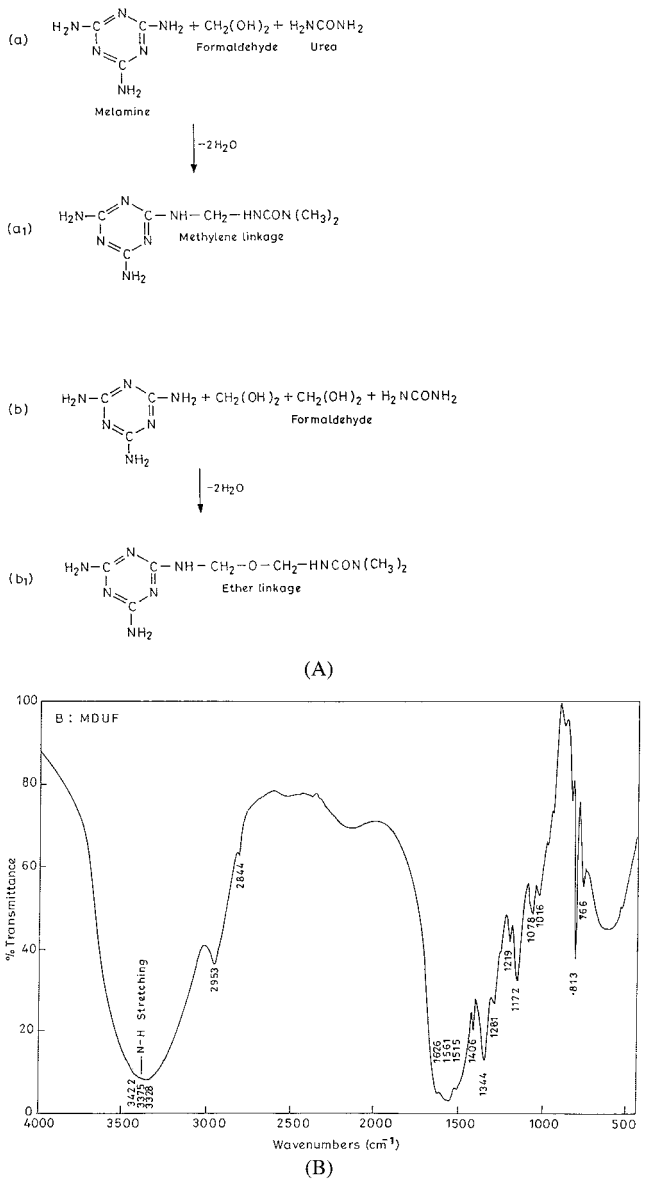

Figure 9 (A) Polycondensation reaction of melamine, dimethylurea, and formaldehyde for MDUF resin preparation; (B) uncured MDUF.

wink equation for molecular weight determination. Various molecular weights of PVOH (poly vinyl alcohol: 45,000, 50,000, 65,000, and 70,000) were used as markers and 54,078 g mol^{-1} average molecular weight was found. Bands at 2953 and 1078 cm^{-1} infer methylene and ether linkages, 1625 and 3375 cm^{-1} bands confirm the presence of –$CONHCH_3$, and >NH. Bands at 3422, 3375, and 3328 cm^{-1} prove the presence of $CON(CH_3)$– stretching with methylene group, and the shoulder at 2844 cm^{-1}, which represents C—H stretching, attributed to asymmetric ($\nu_{as}CH_3$) and symmetric ($\nu_s CH_3$) stretching of CH_3 in and out of phase bending is found at 1406 and 1344 cm^{-1}, thus predicting the presence of CH_3.

CONCLUSIONS

APPS were successfully prepared and adsorption of CO by the strips indicates that CO can be reduced in the atmosphere. The maximum CO was adsorbed by the zero oxidation state of cobalt among transitional metals, Fe in the second oxidation state, and chromium in the third oxidation state.

The authors are extremely grateful to UGC, New Delhi, for financial assistance. Thanks to D. C. Sharama (IIT Delhi) for SEM, D. P. Singh for recording XRF, and P. N. Prasad (IIT Delhi) for tracing work.

References

1. Glasston, S. Phys Chem 1940, 1194.
2. Trruong, et al. J Phys Chem A 2001, 105, 6757.
3. Beeck, O. Trans Faraday Soc 1950, 118.
4. Noggle, J. H. Physical Chemistry, 2nd ed.; Scott, Foresman: Glenview, IL, 1989; pp 298, 309.
5. Noggle, J. H. Physical Chemistry, 2nd ed.; Scott, Foresman: Glenview, IL, 1989; p 508.
6. Helbert, W.; Cavaille, J. Y.; Dufresne, A. Polym Compos 1996, 17, 4.
7. Marchessault, R. H. In: Cellulosics as Advanced Material in Cellulose and Wood Chemistry and Technology; Schuerch, Ed.; Wiley: New York, 1990.
8. Kennedy, J. F.; Phillips.; G. O.; Williams, P. A. In: Cellulose Sources and Exploitation; Chanzy, H., Ed.; Ellis Horwood: New York, 1990; p 3.
9. Borrow, G. M. Physical Chemistry, 5th ed.; McGraw-Hill: New York, 0000; p 278.
10. Noggle, J. H. Physical Chemistry, 2nd ed.; Scott, Foresman: Glenview, IL, 1989; p 5.
11. Phillips, G. O. J Am Chem Soc 1932, 54, 77.
12. Noggle, J. H. Physical Chemistry, 2nd ed.; Scott, Foresman: Glenview, IL, 1989; pp 576–577.
13. Trruong, et al. J Phys Chem A 2001, 105, 6757.
14. Karlsson, J. O.; Blachot, J. F. Polym Compos 1996, 17, 2.
15. Johan, M. F.; Gatenholm, P. Polym Compos 1993, 14, 6.
16. Koper, M. T. M. J Phys Chem B 1999, 103, 26.
17. Gasteiger, H. A.; Markovic, N.; Ross, P. N., Jr.; Cairns, E. J. J Phys Chem 1993, 97, 12020.
18. Gasteiger, H. A.; Markovic, N.; Ross, P. N., Jr.; Cairns, E. J. J Phys Chem 1994, 98, 617.
19. Gasteiger, H. A.; Markovic, N.; Ross, P. N., Jr.; Cairns, E. J. J Electrochem Soc 1994, 141, 1795.
20. Markovic, N.; Gasteiger, H. A.; Ross, P. N., Jr.; Jiang, X.; Villegas, I.; Weaver, M. J Electrochim Acta 1995, 40, 91.
21. Koper, M. J Phys Chem 1994, 98, 617.
22. Weston, R. E. J Phys Chem A 2001, 105, 1656.
23. Hanst, P. L.; Spence, J. W.; Edney, E. O. Atmos Environ 1980, 14, 1077.
24. Logan, J. A.; Prather, M. J.; Wofsy, F. C.; McElroy, M. B. J Geophys Res 1981, 86, 7210.
25. Seiler, W.; Amazionia, C. R.; Dickenson, R. E., Eds. Title of Work; Wiley: New York, 1987; pp 133–160.
26. Ravishankara, A. R. Annu Rev Phys Chem 1988, 39, 367.
27. Johnston, H. S.; Kinnison, D. J Geophys Res 1998, 103, 21967.
28. Watanabe, M.; Zhu.; Y. J Phys Chem B 2000, 104, 1762.
29. Schneider, M. H.; Brebner, K. I. Wood Sci Technol 1985, 19, 67.
30. Nakamura, T.; Okamura, M.; Moriguchi, Y.; Hayase, T. U.S. Pat. 4,404,347 (1983).
31. Goettler, L. A. U.S. Pat. 4,376,144 (1983).
32. Coran, A. Y.; Patel, R. U.S. Pat. 4,323,625 (1982).

33. Beshay, A. D.; Kokta, B. V.; Daneault, C. Polym Compos 1985, 6, 261.
34. Kokta, B. V.; Dambele, F.; Daneault, C. In: Polymer Science and Technology; Carraher, C. E., Jr.; Sperling, L. H., Eds.; Plenum Press: New York, 1985; pp 33, 85.
35. Quick, J. R. ACS Symp Ser 1975, 169, 195.
36. Michell, A. J.; Willis, D. Appita 1978, 31, 347.
37. Michell, A. J.; Willis, D. Appita 1978, 31, 347.
38. Woodhams, R. T.; Thomas, G.; Rodgers, D. K. Polym Eng Sci 1984, 24, 1166.
39. Klason, C.; Kubat, J.; Stromvall, H. E. Int J Polym Mater 1984, 10, 159.
40. Sapieha, S.; Caron, M.; Schreiber, H. P. J Appl Polym Sci 1986, 32, 5663.
41. Kokta, B.; Chen, R.; Daneault, C.; Valade, J. Polym Compos 1983, 4, 229.
42. Czarnecki, L.; White, J. L. J Appl Polym Sci 1980, 25, 1217.
43. Bataille, P.; Allard, P.; Cousin, P. Polym Compos 1990, 11, 5.
44. Helebert, W.; Cavaille, J. Y. Polym Compos 1996, 17, 4.
45. Jenkins, R.; Gould, R. W.; Gedcke, D. Quantitative X-ray Spectrometry; Marcel Dekker: New York, 1981; p 445.